Volume 11
Number 9
7 March 2020
Pages 2305–2574

Chemical Science

rsc.li/chemical-science

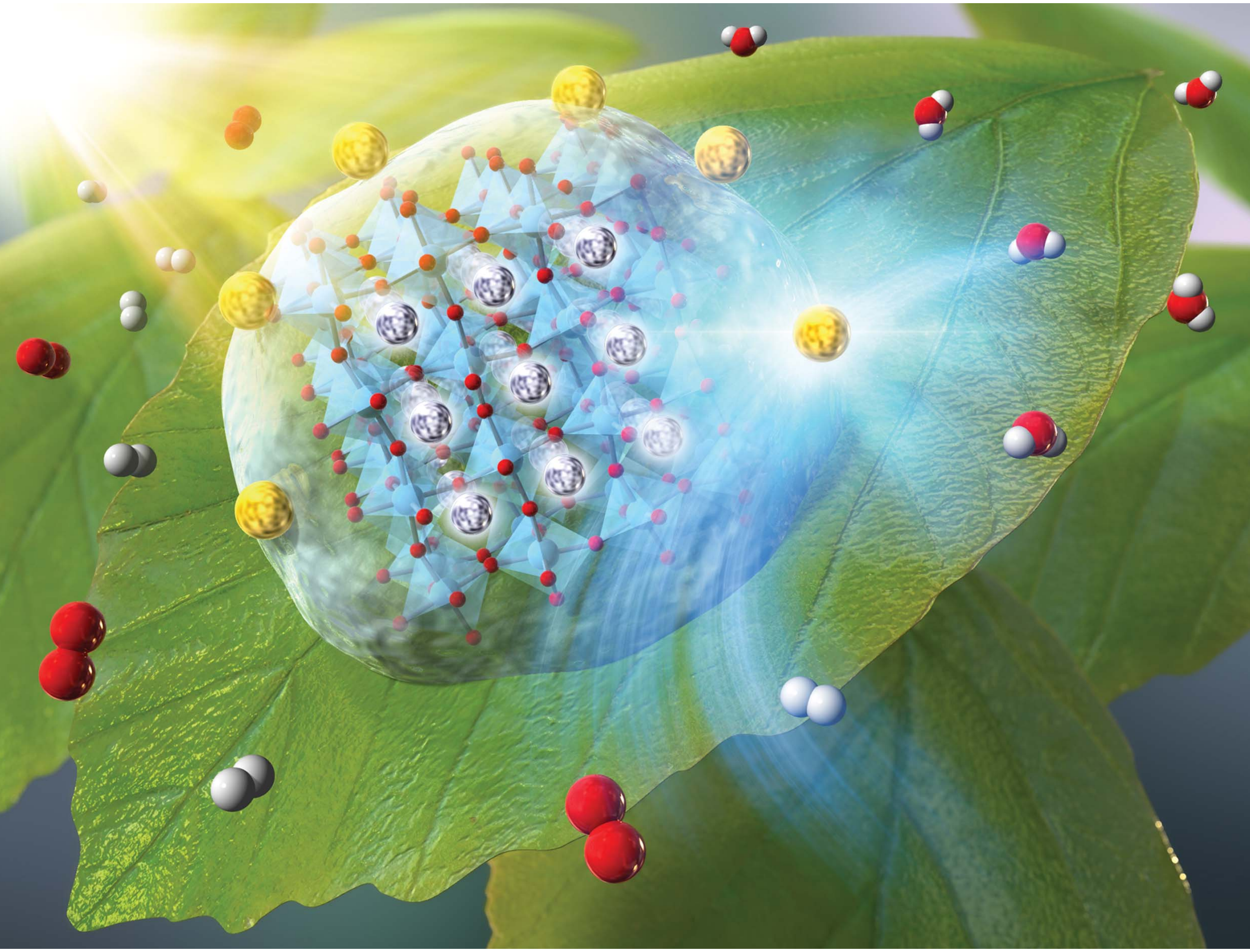

ISSN 2041-6539

ROYAL SOCIETY OF CHEMISTRY

EDGE ARTICLE
Akihiko Kudo *et al.*
Solar water splitting over $Rh_{0.5}Cr_{1.5}O_3$-loaded $AgTaO_3$ of a valence-band-controlled metal oxide photocatalyst

Chemical
Science

ROYAL SOCIETY
OF CHEMISTRY

EDGE ARTICLE

View Article Online
View Journal | View Issue

Check for updates

Cite this: *Chem. Sci.*, 2020, **11**, 2330

All publication charges for this article have been paid for by the Royal Society of Chemistry

Received 21st November 2019
Accepted 28th January 2020

DOI: 10.1039/c9sc05909a

rsc.li/chemical-science

Solar water splitting over $Rh_{0.5}Cr_{1.5}O_3$-loaded $AgTaO_3$ of a valence-band-controlled metal oxide photocatalyst†

Kenta Watanabe,[a] Akihide Iwase [ab] and Akihiko Kudo *[ab]

Improvement of water splitting performance of $AgTaO_3$ (BG 3.4 eV) of a valence-band-controlled photocatalyst was examined. Survey of cocatalysts revealed that a $Rh_{0.5}Cr_{1.5}O_3$ cocatalyst was much more effective than Cr_2O_3, RuO_2, NiO and Pt for water splitting into H_2 and O_2 in a stoichiometric amount. The optimum loading amount of the $Rh_{0.5}Cr_{1.5}O_3$ cocatalyst was 0.2 wt%. The apparent quantum yield (AQY) at 340 nm of the optimized $Rh_{0.5}Cr_{1.5}O_3$(0.2 wt%)/$AgTaO_3$ photocatalyst reached to about 40%. $Rh_{0.5}Cr_{1.5}O_3$(0.2 wt%)/$AgTaO_3$ gave a solar to hydrogen conversion efficiency (STH) of 0.13% for photocatalytic water splitting under simulated sunlight irradiation. Bubbles of gasses evolved by the solar water splitting were visually observed under atmospheric pressure at room temperature.

Introduction

Photocatalytic solar water splitting is an important reaction because it has the potential for solving resources, energy and environmental issues. Hence, many researchers have aimed to develop water splitting systems of a one-step photoexcitation type and a two-step photoexcitation type (Z-scheme) with visible-light-driven powdered photocatalysts.[1–6] The simplicity of the one-step photoexcitation type will be an advantage in practical use. Domen and co-workers have reported that (oxy)nitride and oxysulfide photocatalysts such as GaN–ZnO,[7,8] $ZnGeN_2$–ZnO,[9,10] $LaMg_{1/3}Ta_{2/3}O_2N$,[11–13] TaON,[14] $CaTaO_2N$,[15] Ta_3N_5 (ref. 16) and $Y_2Ti_2O_5S_2$ (ref. 17) show activities for one-step photoexcitation type water splitting under visible light irradiation. We have also reported that Rh,Sb-codoped $SrTiO_3$ of a metal oxide photocatalyst shows the water splitting activity under visible light irradiation by loading of an IrO_2 cocatalyst.[18] Although above visible-light-responsive photocatalysts split water under sunlight irradiation, their solar energy conversion efficiencies (solar to hydrogen conversion efficiency, STH) do not reach the level for practical use due to low apparent quantum yields (AQY). In terms of the high AQY, NiO-loaded La-doped $NaTaO_3$ (ref. 19) (BG 4.1 eV), $Rh_{0.5}Cr_{1.5}O_3$-loaded Zn,Ca-codoped Ga_2O_3 (ref. 20) (BG 4.6 eV) and MoO_y,$RhCrO_x$-coloaded Al-doped $SrTiO_3$ (ref. 21) (BG 3.2 eV) show the AQYs of 56% at 270 nm, 71% at 254 nm and 69% at 365 nm, for photocatalytic water splitting under UV irradiation, respectively. However, only Al-doped $SrTiO_3$ can respond to sunlight ($\lambda > 300$ nm) with STH of 0.4%.[22] Thus, the development of sunlight-driven photocatalysts with one-step photoexcitation for water splitting is an important research topic.

We have reported that a $AgTaO_3$ photocatalyst (BG 3.4 eV) shows water splitting activity under UV irradiation by loading of a NiO cocatalyst.[23] The characteristics of $AgTaO_3$ is the valence band maximums formed by Ag 4d orbitals which are located above the bands formed by O 2p orbitals, and hence the band gap of $AgTaO_3$ is relatively narrow among the metal oxides containing Ta. $AgTaO_3$ is expected to respond to sunlight judging from the band gap of 3.4 eV, while the water splitting under sunlight irradiation has not been achieved yet. Moreover, the crystal structure of perovskite for $AgTaO_3$ is the same as that for $SrTiO_3$ and $NaTaO_3$ photocatalysts with high activities for water splitting. These backgrounds motivate us to investigate solar water splitting using the $AgTaO_3$ photocatalyst.

A cocatalyst is one of the most effective factors for improvement of the photocatalytic activity. Actually, the water splitting activity of $AgTaO_3$ is drastically improved by loading of a NiO cocatalyst which is widely used in water splitting over metal oxides.[23] Recently, $Rh_{0.5}Cr_{1.5}O_3$ has also arisen as a potential candidate cocatalyst for water splitting over metal oxides.[20,21] In the present study, we investigated the loading effect of various cocatalysts on water splitting over $AgTaO_3$. Solar water splitting was also demonstrated using the $AgTaO_3$ with the optimized cocatalyst.

Experimental

Preparation of photocatalysts

$AgTaO_3$ was synthesized by a solid-state reaction using Ag_2O (Kanto Chemical; 99.0%) and Ta_2O_5 (Rare Metallic; 99.99%) as

---

[a] *Department of Applied Chemistry, Faculty of Science, Tokyo University of Science, 1-3 Kagurazaka, Shinjuku-ku, Tokyo 162-8601, Japan. E-mail: a-kudo@rs.tus.ac.jp*

[b] *Photocatalysis International Research Center, Research Institute for Science and Technology, Tokyo University of Science, 2641 Yamazaki, Noda-shi, Chiba-ken 278-8510, Japan*

† Electronic supplementary information (ESI) available. See DOI: 10.1039/c9sc05909a

starting materials. The starting materials were mixed in an alumina mortar in a ratio of Ag : Ta = 1 + x : 1 (x = 0, 0.03, 0.05, 0.07). The mixture was calcined in air at 1173–1373 K for 5–20 h in an alumina crucible. The calcined materials were washed with 1 mol L^{-1} of an aqueous HNO_3 solution in ultrasonication for 1 h in order to remove Ag metals deposited on the surface of $AgTaO_3$.

A Pt cocatalyst was loaded *in situ* by a photodeposition method using an aqueous H_2PtCl_6 (Tanaka Kikinzoku; 37.7 wt% as Pt) solution. NiO,[23] RuO_2 (ref. 24) and Cr_2O_3 (ref. 25) of cocatalysts were loaded on $AgTaO_3$ photocatalysts by an impregnation method using $Ni(NO_3)_2 \cdot 6H_2O$ (Wako Pure Chemical; 98.0%), $Ru_3(CO)_{12}$ (Aldrich; 99%), $Cr(NO_3)_3 \cdot 9H_2O$ (Kanto Chemical; 98.0–103.0%). $AgTaO_3$ powder was suspended in aqueous solutions dissolving $Ni(NO_3)_2$ or $Cr(NO_3)_3$, and an acetone solution dissolving $Ru_3(CO)_{12}$ in porcelain crucibles. The $AgTaO_3$-suspended solutions were dried up on a water bath and subsequently calcined in an electric furnace with conditions of 543 K – 1 h for NiO, 673 K – 2 h for RuO_2 and 623 K – 1 h for Cr_2O_3. $Rh_{0.5}Cr_{1.5}O_3$ (ref. 25) cocatalyst was loaded by a simple impregnation method using $Cr(NO_3)_3 \cdot 9H_2O$ and $Rh(NO_3)_3$ (Kanto Chemical; >80.0% as anhydrous). $AgTaO_3$-suspended aqueous solution containing both $Rh(NO_3)_3$ and $Cr(NO_3)_3$ was dried up and subsequently calcined at 623 K for 1 h. It is reported that $Rh_{0.5}Cr_{1.5}O_3$ of a mixed oxide is naturally formed on a photocatalyst by this process.[26] The loading amount of $Rh_{0.5}Cr_{1.5}O_3$ was controlled by adjusting the amount of starting materials.

Characterization

The crystal structure of the synthesized $AgTaO_3$ was identified by powder X-ray diffraction (Rigaku; MiniFlex600). The elemental composition of the synthesized $AgTaO_3$ was measured by an X-ray fluorescence spectrometer (Rigaku; NEX DE). A Diffuse reflectance spectrum was measured using a UV-vis-NIR spectrometer with an integrating sphere (Jasco; UbeatV-570) and was converted from reflection to absorbance mode by the Kubelka–Munk method. Morphologies of photocatalyst particles and $Rh_{0.5}Cr_{1.5}O_3$-cocatalysts were observed using a scanning electron microscope (JEOL; JSM-7400F) and a transmission electron microscope (JEOL; JEM-2100F). A chemical state of Rh in $Rh_{0.5}Cr_{1.5}O_3$-loaded $AgTaO_3$ was analyzed using an X-ray photoelectron spectroscopy (JEOL; JPS-9010MC).

Photocatalytic reaction

Photocatalytic water splitting was carried out in a gas-closed-circulation system. Photocatalyst powder (0.3 g) was dispersed in distilled water (120 mL) in a top-irradiation cell with a Pyrex window. A 300 W Xe-arc lamp (PerkinElmer; Cermax-PE300BF) and a solar simulator (Asahi spectra; HAL-320) were employed as a light source. An inner-irradiation reaction cell made of quartz equipped with a 400 W high-pressure Hg lamp (SEN; HL400EH-5) was also used for photocatalytic water splitting in order to compare with the activity of NiO/$NaTaO_3$:La.[19] Amounts of evolved H_2 and O_2 gases were determined with a gas chromatograph (Shimadzu; GC-8A, MS-5A, Ar carrier gas, TCD). Turnover number (TON) of the amount of reacted electrons/holes to the molar quantity of $AgTaO_3$ was estimated using the eqn (1).

$$\begin{aligned}[\text{TON}] &= [\text{the molar quantity of reacted electrons}]/[\text{the molar quantity of } AgTaO_3] \\ &= [(\text{the amount of evolved } H_2) \times 2/\text{mol}]/[\text{the molar quantity of } AgTaO_3/\text{mol}] \end{aligned} \quad (1)$$

Apparent quantum yields (AQY) were measured using a 300 W Xe-arc lamp (Asahi Spectra; MAX-302) with band-pass filters (Asahi Spectra). The photon flux of the monochromatic light through the long-pass filters was measured using a silicon diode head (OPHIR; PD300-UV head and NOVA display). An AQY and a solar to hydrogen conversion efficiency (STH) were estimated using the following eqn (2) and (3).

$$\begin{aligned}[\text{AQY}\%] &= 100 \times [\text{the number of reacted electrons or holes}]/[\text{the number of incident photons}] \\ &= 100 \times [(\text{the number of evolved } H_2 \text{ molecules}) \times 2]/[\text{the number of incident photons}] \end{aligned} \quad (2)$$

$$\begin{aligned}[\text{STH}\%] &= 100 \times ([\Delta G^0(H_2O)/\text{kJ mol}^{-1}] \times [\text{rate of } H_2 \text{ evolution}/\mu\text{mol h}^{-1}])/([\text{irradiation time/s}] \\ &\quad \times [\text{solar energy (AM1.5G)/mW cm}^{-2}] \times [\text{irradiation area/cm}^2]) \\ &= (237 \times [\text{rate of } H_2 \text{ evolution}/\mu\text{mol h}^{-1}])/(3600 \times 100 \times 25) \times 100 \end{aligned} \quad (3)$$

Results and discussion

XRD measurement confirmed that trigonal $AgTaO_3$ with a perovskite structure was successfully synthesized in a single phase as previously reported (Fig. S1†).[23] The peaks due to metallic Ag were not observed in XRD patterns of $AgTaO_3$ both before and after washing with an aqueous HNO_3 solution. However, the absorption due to the surface plasmonic resonance of Ag was observed in diffuse reflectance spectra of the $AgTaO_3$ before and after the washing (Fig. S2†). The absorption due to the surface plasmonic resonance after the washing was a little bit smaller than that before the washing. Therefore, metallic Ag on the surface would be removed by the washing but the amount of removed Ag was quite small. Actually, atomic ratios of Ag to Ta in the $AgTaO_3$ after the washing were calculated to be 1.00 and 0.99 from XPS and XRF measurements, respectively. These results indicate that the ratios of Ag to Ta on the surface and in the bulk were almost stoichiometric even if after the washing. The absorption edge of $AgTaO_3$ was around 380 nm in a diffuse reflectance spectrum (Fig. S3†), indicating 3.4 eV of the band gap. Scanning electron microscope observation revealed that the size of $AgTaO_3$ particles was from several hundreds nm to several μm (Fig. S4†).

Table 1 shows the activities for photocatalytic water splitting over $AgTaO_3$ loaded with various cocatalysts under UV irradiation. Non-loaded $AgTaO_3$ produced only a small amount of H_2

Table 1 Photocatalytic water splitting over $AgTaO_3$ loaded with various cocatalysts under UV irradiation[a]

Cocatalyst (wt%)	Loading method	Activity/μmol h^{-1}	
		H_2	O_2
None	—	0.5	0
$Rh_{0.5}Cr_{1.5}O_3$ (0.05)	Impregnation (623 K – 1 h)	56	28
$Rh_{0.5}Cr_{1.5}O_3$ (0.1)	Impregnation (623 K – 1 h)	318	162
$Rh_{0.5}Cr_{1.5}O_3$ (0.2)	Impregnation (623 K – 1 h)	400	192
$Rh_{0.5}Cr_{1.5}O_3$ (0.3)	Impregnation (623 K – 1 h)	217	111
Cr_2O_3 (0.13)	Impregnation (623 K – 1 h)	1.8	0.9
RuO_2 (0.2)	Impregnation (673 K – 2 h)	1.6	0.5
NiO (0.2)	Impregnation (543 K – 1 h)	18	4
Pt (0.2)	Photodeposition (*in situ*)	45	4

[a] Photocatalyst: 0.3 g, reactant solution: distilled water (120 mL), cell: top-irradiation cell with a Pyrex window, light source: 300 W Xe-arc lamp ($\lambda > 300$ nm).

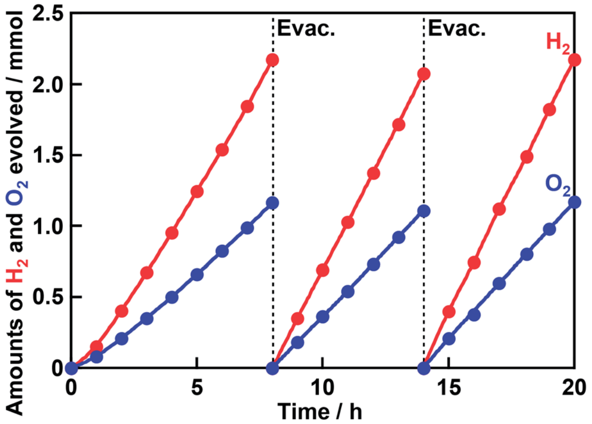

Fig. 1 Photocatalytic water splitting over $Rh_{0.5}Cr_{1.5}O_3$(0.2 wt%)/$AgTaO_3$. $AgTaO_3$ was synthesized by a solid state reaction at 1273 K for 15 h without excess Ag. $Rh_{0.5}Cr_{1.5}O_3$ was loaded by an impregnation method at 623 K for 1 h. Photocatalyst: 0.3 g, reactant solution: distilled water (120 mL), cell: top-irradiation cell with a Pyrex window, light source: 300 W Xe-arc lamp ($\lambda > 300$ nm).

without O_2 evolution. In other words, water splitting did not proceed. In contrast, all $AgTaO_3$ loaded with various cocatalysts produced both H_2 and O_2. However, the amount of evolved H_2 was more than a stoichiometric amount when NiO, RuO_2 and Pt were loaded. When Cr_2O_3 and $Rh_{0.5}Cr_{1.5}O_3$ were loaded, the stoichiometric amounts of H_2 and O_2 evolved, indicating that ideal water splitting proceeded. In particular, the activity of $AgTaO_3$ was greatly improved by loading of the $Rh_{0.5}Cr_{1.5}O_3$ cocatalyst. This result is appropriate because $Rh_{0.5}Cr_{1.5}O_3$ is known as an effective cocatalyst for photocatalytic water splitting. It is reported that Cr_2O_3 does not work as a cocatalyst for photocatalytic water splitting but Ag coloaded with Cr works as a cocatalyst.[25] In the present case, only Cr_2O_3-loaded $AgTaO_3$ showed the water splitting activity. This is probably because a small amount of metallic Ag still remained on the surface of $AgTaO_3$ even after washing with an aqueous HNO_3 solution and a Ag–Cr cocatalyst was formed by loading of Cr_2O_3 as an effective cocatalyst. We optimized the loading amount of the $Rh_{0.5}Cr_{1.5}O_3$ cocatalyst and synthesis conditions of $AgTaO_3$. The water splitting activity of $AgTaO_3$ slightly depended on synthesis conditions and 1273 K – 15 h was the best condition for the activity (Table S1†). In addition, the activity was insensitive for addition of an excess amount of Ag. On the other hand, the activity much depended on the loading amount of $Rh_{0.5}Cr_{1.5}O_3$ cocatalyst and 0.2 wt% was optimum (Table 1). The optimized $Rh_{0.5}Cr_{1.5}O_3$(0.2 wt%)/$AgTaO_3$ stably and continuously produced H_2 and O_2 using a Xe lamp (Fig. 1).

Chemical and physical states of the loaded $Rh_{0.5}Cr_{1.5}O_3$ in $Rh_{0.5}Cr_{1.5}O_3$(0.2 wt%)/$AgTaO_3$ before and after water splitting were characterized using a transmission electron microscope (TEM) and an X-ray photoelectron spectroscopy (XPS) because the water splitting activity of $AgTaO_3$ was greatly improved by loading a $Rh_{0.5}Cr_{1.5}O_3$ cocatalyst. It was confirmed by TEM that $Rh_{0.5}Cr_{1.5}O_3$ particles with a diameter of about 10–20 nm were loaded on $AgTaO_3$ (Fig. 2), as observed for GaN–ZnO.[26] In XPS spectra, the binding energy of the Rh $3d_{5/2}$ peak for $Rh_{0.5}Cr_{1.5}O_3$(0.2 wt%)/$AgTaO_3$ was 309.0 eV (Fig. S5†) which is close to not that for Rh_2O_3 (308.3 eV) but that for $Rh_{0.5}Cr_{1.5}O_3$ (308.9 eV).[26] The slightly positive shift in the binding energy was also observed for the $Rh_{0.5}Cr_{1.5}O_3$ loaded on GaN–ZnO (309.1 eV).[26] These results indicate that the loaded $Rh_{0.5}Cr_{1.5}O_3$ on $AgTaO_3$ in the present study was similar to that on GaN–ZnO. Additionally, the TEM image of $Rh_{0.5}Cr_{1.5}O_3$ cocatalysts did not change so much after photocatalytic water splitting. On the other hand, in the XPS spectra, the Rh $3d_{5/2}$ peak for $Rh_{0.5}Cr_{1.5}O_3$(0.2 wt%)/$AgTaO_3$ after photocatalytic water splitting was broadened to lower binding energy than that before photocatalytic water splitting. This observation indicated that the photocatalyst was activated by partial reduction of Rh in loaded $Rh_{0.5}Cr_{1.5}O_3$ cocatalyst to the metallic form during the induction period in Fig. 1.

An action spectrum of water splitting on the optimized $Rh_{0.5}Cr_{1.5}O_3$(0.2 wt%)/$AgTaO_3$ was measured, as shown in Fig. 3. The maximum AQY was 38% at 340 nm. As far as we know, the AQY is the highest among one-step photoexcitation type water splitting using metal oxide photocatalysts with valence bands consisting of metal cation orbitals. In order to compare the activity of $Rh_{0.5}Cr_{1.5}O_3$(0.2 wt%)/$AgTaO_3$ with that

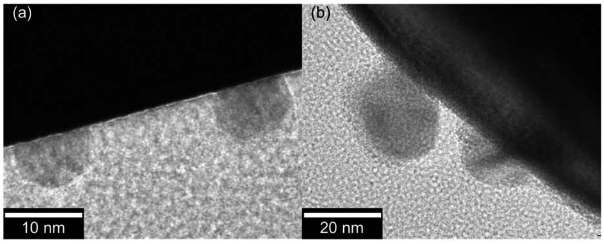

Fig. 2 TEM images of $Rh_{0.5}Cr_{1.5}O_3$(0.2 wt%)/$AgTaO_3$ (a) before and (b) after photocatalytic water splitting under UV irradiation using a 300 W Xe-arc lamp. $AgTaO_3$ was synthesized by a solid state reaction at 1273 K for 15 h without excess Ag. $Rh_{0.5}Cr_{1.5}O_3$ was loaded by an impregnation method at 623 K for 1 h.

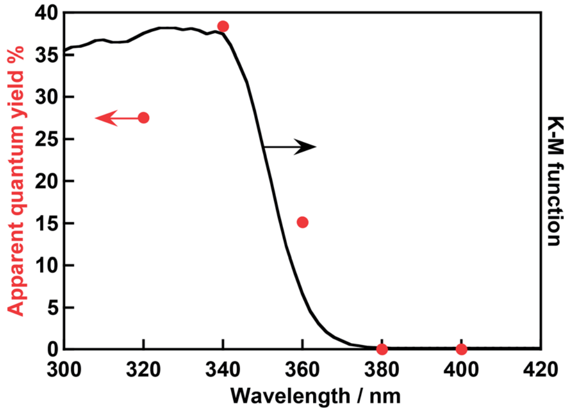

Fig. 3 An action spectrum of water splitting over $Rh_{0.5}Cr_{1.5}O_3$(0.2-wt%)/$AgTaO_3$ and a diffuse reflectance spectrum of $AgTaO_3$ prepared by a solid state reaction at 1273 K for 15 h without excess Ag. $Rh_{0.5}Cr_{1.5}O_3$ was loaded by an impregnation method at 623 K for 1 h. Photocatalyst: 0.3 g, reactant solution: distilled water (120 mL), cell: top-irradiation cell with a Pyrex window, light source: 300 W Xe-arc lamp with band-pass filters.

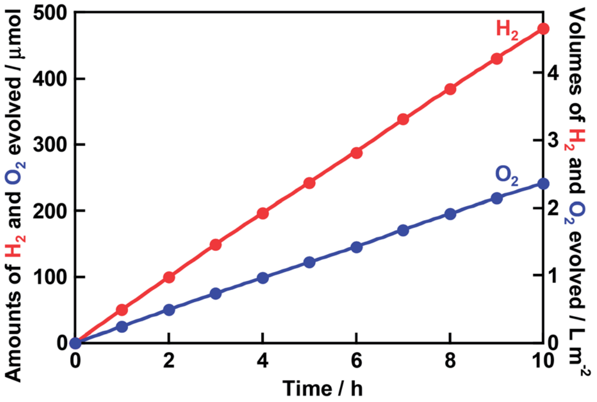

Fig. 5 Photocatalytic solar water splitting over $Rh_{0.5}Cr_{1.5}O_3$(0.2 wt%)/$AgTaO_3$. $AgTaO_3$ was synthesized by a solid state reaction at 1273 K for 15 h without excess Ag. $Rh_{0.5}Cr_{1.5}O_3$ was loaded by an impregnation method at 623 K for 1 h. $Rh_{0.5}Cr_{1.5}O_3$(0.2 wt%)/$AgTaO_3$ was activated by a 300 W Xe-arc lamp in distilled water for 20 h before this reaction (Fig. 1) in order to eliminate the induction period early. Photocatalyst: 0.3 g, reactant solution: distilled water (120 mL), cell: top-irradiation cell with a Pyrex window, light source: a solar simulator with an AM1.5-filter (100 mW cm^{-2}), irradiation area: 25 cm^2.

of highly active NiO/$NaTaO_3$:La, photocatalytic water splitting over $Rh_{0.5}Cr_{1.5}O_3$(0.2 wt%)/$AgTaO_3$ was carried out in an inner-irradiation reaction cell made of quartz equipped with a 400 W high pressure Hg-lamp using 1 g of photocatalyst powder suspended in 340 mL of distilled water, as shown in Fig. 4. Evolution rates of H_2 and O_2 were 20 mmol h^{-1} and 10 mmol h^{-1}, respectively. The activity of $Rh_{0.5}Cr_{1.5}O_3$(0.2 wt%)/$AgTaO_3$ was similar to that of NiO/$NaTaO_3$:La.[19] This reaction catalytically proceeded because TON was 47. Thus, $Rh_{0.5}Cr_{1.5}O_3$(0.2-wt%)/$AgTaO_3$ interestingly showed the high activity for water splitting even without doping unlike La-doped $NaTaO_3$, Zn,Ca-codoped Ga_2O_3, and Al-doped $SrTiO_3$, suggesting that $AgTaO_3$ itself has good potential for water splitting. One possible explanation about the potential of $AgTaO_3$ will be the distortion of its crystal structure. The Ta–O–Ta bond angle of $AgTaO_3$ (164 degree) is very similar to that of $NaTaO_3$ (163 degree).[23] The similarity in the lattice distortion between $AgTaO_3$ and $NaTaO_3$ causes a similar property of a conduction band of $AgTaO_3$ to a highly active $NaTaO_3$. Therefore, mobility of photogenerated electrons and a reduction potential of water reduction of $AgTaO_3$ should be similar to those of $NaTaO_3$. Additionally, the valence band of $NaTaO_3$ is formed by only O 2p orbitals, whereas that of $AgTaO_3$ is formed by hybridized orbitals between Ag 4d and O 2p.[23] Therefore, photogenerated holes in $AgTaO_3$ could migrate more easily than those in $NaTaO_3$. These positive factors in $AgTaO_3$ gave high photocatalytic activity.

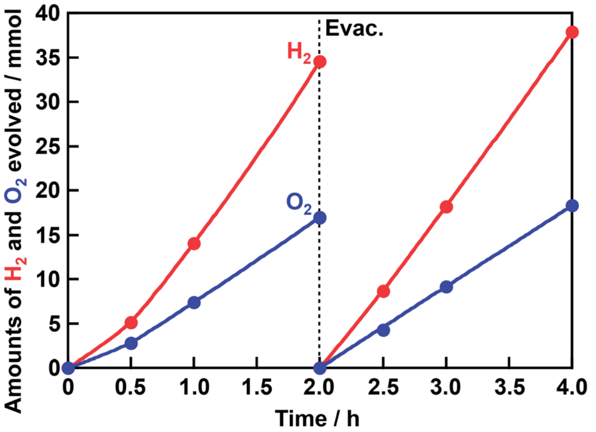

Fig. 4 Photocatalytic water splitting over $Rh_{0.5}Cr_{1.5}O_3$(0.2 wt%)/$AgTaO_3$ under UV irradiation. Photocatalyst: 1 g, reactant solution: distilled water (340 mL), cell: inner-irradiation cell made of quartz, light source: 400 W high pressure Hg-lamp. $AgTaO_3$ was synthesized by a solid state reaction at 1273 K for 15 h without excess Ag. $Rh_{0.5}Cr_{1.5}O_3$ was loaded by an impregnation method at 623 K for 1 h.

Water splitting proceeded over the $Rh_{0.5}Cr_{1.5}O_3$(0.2 wt%)/$AgTaO_3$ photocatalyst even under simulated sunlight irradiation, as shown in Fig. 5. H_2 and O_2 were steadily evolved with the rates of 486 mL m^{-2} h^{-1} and 247 mL m^{-2} h^{-1}, respectively. The STH was estimated to be 0.13%. Additionally, we were able to watch evolved bubbles when $Rh_{0.5}Cr_{1.5}O_3$(0.2 wt%)/$AgTaO_3$ on the bottom of the reaction cell was irradiated with simulated sunlight under 1 atm at room temperature. The STH of $Rh_{0.5}Cr_{1.5}O_3$(0.2-wt%)/$AgTaO_3$ is lower than those of TiO_2/CoOOH/$RhCrO_x$/$SrTiO_3$:Al (STH = 0.4%)[22] and $SrTiO_3$:Rh,La-Au-$BiVO_4$:Mo photocatalyst sheet (STH = 1.1%),[27] whereas it is higher than those of Z-schematic water splitting using $SrTiO_3$:Rh of a H_2-evolving photocatalyst, $BiVO_4$ of an O_2-evolving photocatalyst, and ionic electron mediators such as $Fe^{3+/2+}$ and $[Co(bpy)_3]^{3+/2+}$.[28,29] Thus, we successfully achieved highly efficient one-step photoexcitation type solar water splitting using $Rh_{0.5}Cr_{1.5}O_3$(0.2 wt%)/$AgTaO_3$ of a valence-band-controlled metal oxide photocatalyst.

Conclusions

$Rh_{0.5}Cr_{1.5}O_3$(0.2 wt%)-loaded $AgTaO_3$ has arisen as a photocatalyst for solar water splitting in a suspension system. The

AQY of $Rh_{0.5}Cr_{1.5}O_3$(0.2 wt%)/$AgTaO_3$ was about 40% at 340 nm. The activity of $Rh_{0.5}Cr_{1.5}O_3$(0.2 wt%)/$AgTaO_3$ was similar to that of NiO/$NaTaO_3$:La under the same experimental condition, using 1 g of photocatalyst powder suspended in 340 mL of distilled water, in an inner-irradiation cell made of quartz equipped with a 400 W high pressure Hg-lamp. $AgTaO_3$ seems to have good potential for water splitting because $Rh_{0.5}Cr_{1.5}O_3$(0.2 wt%)/$AgTaO_3$ showed the high AQY even without doping of elements. $Rh_{0.5}Cr_{1.5}O_3$(0.2 wt%)/$AgTaO_3$ also showed the photocatalytic activity for water splitting under simulated sunlight irradiation with the STH of 0.13%. The AQY and STH of $Rh_{0.5}Cr_{1.5}O_3$(0.2 wt%)/$AgTaO_3$ were the highest for one-step photoexcitation type water splitting using a valence-band-controlled metal oxide photocatalyst. Thus, it was clarified that a metal oxide photocatalyst with a valence band consisting of metal cation orbitals rather than O 2p could be utilized as a photocatalyst for highly efficient water splitting. The knowledge is expected to be applied to visible-light-driven photocatalysts.

Conflicts of interest

There are no conflicts to declare.

Acknowledgements

This work was supported by JSPS KAKENHI Grant Numbers 17H06433 in Scientific Research on Innovative Areas "Innovations for Light-Energy Conversion (I^4LEC)" and 17H0127. The authors gratefully thank Dr T. Ichihashi for assistance with TEM measurements.

Notes and references

1 F. E. Osterloh, *Chem. Mater.*, 2008, **20**, 35–54.
2 Y. Inoue, *Energy Environ. Sci.*, 2009, **2**, 364–386.
3 A. Kudo and Y. Miseki, *Chem. Soc. Rev.*, 2009, **38**, 253–278.
4 R. Abe, *J. Photochem. Photobiol., C*, 2010, **11**, 179–209.
5 T. Hisatomi, J. Kubota and K. Domen, *Chem. Soc. Rev.*, 2014, **43**, 7520–7535.
6 K. Maeda and K. Domen, *Bull. Chem. Soc. Jpn.*, 2016, **89**, 627–648.
7 K. Maeda, T. Takata, M. Hara, N. Saito, Y. Inoue, H. Kobayashi and K. Domen, *J. Am. Chem. Soc.*, 2005, **127**, 8286–8287.
8 K. Maeda, K. Teramura, D. Lu, T. Takata, N. Saito, Y. Inoue and K. Domen, *Nature*, 2006, **440**, 295.
9 Y. Lee, H. Terashima, Y. Shimodaira, K. Teramura, M. Hara, H. Kobayashi, K. Domen and M. Yashima, *J. Phys. Chem. C*, 2007, **111**, 1042–1048.
10 K. Takanabe, T. Uzawa, X. Wang, K. Maeda, M. Katayama, J. Kubota, A. Kudo and K. Domen, *Dalton Trans.*, 2009, 10055–10062.
11 C. Pan, T. Takata, M. Nakabayashi, T. Matsumoto, N. Shibata, Y. Ikuhara and K. Domen, *Angew. Chem., Int. Ed.*, 2015, **54**, 2955–2959.
12 C. Pan, T. Takata and K. Domen, *Chem.–Eur. J.*, 2016, **22**, 1854–1862.
13 C. Pan, T. Takata, K. Kumamoto, T. Minegishi, M. Nakabayashi, T. Matsumoto, N. Shibata, Y. Ikuhara and K. Domen, *J. Mater. Chem. A*, 2016, **4**, 4544–4552.
14 K. Maeda, D. Lu and K. Domen, *Chem.–Eur. J.*, 2013, **19**, 4986–4991.
15 J. Xu, C. Pan, T. Takata and K. Domen, *Chem. Commun.*, 2015, **51**, 7191–7194.
16 Z. Wang, Y. Inoue, T. Hisatomi, R. Ishikawa, Q. Wang, T. Takata, S. Chen, N. Shibata, Y. Ikuhara and K. Domen, *Nat. Catal.*, 2018, **1**, 756–763.
17 Q. Wang, M. Nakabayashi, T. Hisatomi, S. Sun, S. Akiyama, Z. Wang, Z. Pan, X. Xiao, T. Watanabe, T. Yamada, N. Shibata, T. Takata and K. Domen, *Nat. Mater.*, 2019, **18**, 827–832.
18 R. Asai, H. Nemoto, Q. Jia, K. Saito, A. Iwase and A. Kudo, *Chem. Commun.*, 2014, **50**, 2543–2546.
19 H. Kato, K. Asakura and A. Kudo, *J. Am. Chem. Soc.*, 2003, **125**, 3082–3089.
20 Y. Sakata, T. Hayashi, R. Yasunaga, N. Yanaga and H. Imamura, *Chem. Commun.*, 2015, **51**, 12935–12938.
21 H. T. Chiang, H. Lyu, T. Hisatomi, Y. Goto, T. Takata, M. Katayama, T. Minegishi and K. Domen, *ACS Catal.*, 2018, **8**, 2782–2788.
22 H. Lyu, T. Hisatomi, Y. Goto, M. Yoshida, T. Higashi, M. Katayama, T. Takata, T. Minegishi, H. Nishiyama, T. Yamada, Y. Sakata, K. Asakura and K. Domen, *Chem. Sci.*, 2019, **10**, 3196–3201.
23 H. Kato, H. Kobayashi and A. Kudo, *J. Phys. Chem. B*, 2002, **106**, 12441–12447.
24 Y. Inoue, *Energy Environ. Sci.*, 2009, **2**, 364–386.
25 K. Maeda, K. Teramura, N. Saito, Y. Inoue and K. Domen, *J. Catal.*, 2006, **243**, 303–308.
26 K. Maeda, K. Teramura, D. Lu, T. Takata, N. Saito, Y. Inoue and K. Domen, *J. Phys. Chem. B*, 2006, **110**, 13753–13758.
27 Q. Wang, T. Hisatomi, Q. Jia, H. Tokudome, M. Zhong, C. Wang, Z. Pan, T. Takata, M. Nakabayashi, N. Shibata, Y. Li, I. D. Sharp, A. Kudo, T. Yamada and K. Domen, *Nat. Mater.*, 2016, **15**, 611–615.
28 Y. Sasaki, H. Kato and A. Kudo, *J. Am. Chem. Soc.*, 2013, **135**, 5441–5449.
29 H. Kato, Y. Sasaki, N. Shirakura and A. Kudo, *J. Mater. Chem. A*, 2013, **1**, 12327–12333.